Unraveling the Posterolateral Corner of the Knee[1]

Humberto G. Rosas, MD

Abbreviations: LCL = lateral collateral ligament, PFL = popliteofibular ligament, PLC = posterolateral corner

RadioGraphics 2016; 36:1776–1791

Published online 10.1148/rg.2016160027

Content Codes: MK MR

[1]From the Department of Radiology, University of Wisconsin School of Medicine and Public Health, 600 Highland Ave, Madison, WI 53792-3252. Received February 22, 2016; revision requested March 31 and received May 17; accepted June 1. For this journal-based SA-CME activity, the author, editor, and reviewers have disclosed no relevant relationships. **Address correspondence** to the author (e-mail: *hrosas@uwhealth.org*).

SA-CME LEARNING OBJECTIVES

After completing this journal-based SA-CME activity, participants will be able to:

- Identify the major anatomic structures of the PLC of the knee.
- Discuss the biomechanics of the PLC and the consequences of unrecognized injuries.
- Correctly diagnose injuries of the PLC.

See www.rsna.org/education/search/RG.

Although rare, posterolateral corner (PLC) injuries can result in sustained instability and failed cruciate ligament reconstruction if they are not diagnosed. The anatomy of the PLC was once thought to be perplexing and esoteric—in part because of the varying nomenclature applied to this region in the literature, which added unnecessary complexity. More recently, three major structures have been described as the primary stabilizers of the PLC on the basis of biomechanical study findings: the lateral collateral ligament, popliteus tendon, and popliteofibular ligament. An understanding of the anatomic relationships of these structures with each other and with the surrounding osseous structures is invaluable for improving the diagnostic accuracy of magnetic resonance (MR) imaging in the detection of PLC injuries and allowing a structured and systematic approach when interpreting the imaging findings. The majority of PLC injuries do not occur in isolation and are part of a more complex injury pattern that typically involves other vital supporting structures such as the cruciate ligaments, menisci, and medial ligamentous structures. Therefore, imaging has an ever-increasing role in the recognition of these injuries, as the clinical findings may be difficult to interpret adequately owing to synchronous injuries that dominate the physical examination findings. Furthermore, the diagnosis of acute high-grade PLC injuries is critical because early and aggressive treatment, for which surgical reconstruction is often required, leads to improved long-term outcomes and the prevention of persistent instability that would otherwise result in varus thrust gait, chronic pain, and accelerated cartilage damage.

Introduction

The posterolateral corner (PLC) was once regarded as the "dark side of the knee" owing to the complex and variable anatomy superimposed on the inconsistent terminology used in the literature to describe the structures in this region. Although infrequent, injuries to the PLC can lead to devastating consequences, including chronic knee instability, cartilage damage, and failed cruciate ligament reconstruction, if they are not detected. Timely diagnosis and surgical intervention are imperative for improving long-term outcomes.

The increased awareness and recognition of these previously elusive injuries can be attributed to recent studies in which the fine anatomic detail of this region was elucidated and defined, as well as advancements in imaging. In this article, we review the anatomy, biomechanics, imaging appearances, and injury patterns of the PLC in hopes of demystifying this region of the knee.

TEACHING POINTS

- The structures of the PLC are primarily responsible for resisting varus angulation—sometimes referred to as *varus rotation*—and external tibial rotation. They act as secondary stabilizers, in conjunction with the cruciate ligaments, to prevent anterior and posterior translation during the early phase of flexion (0°–30°).
- Rarely seen in isolation, the majority of high-grade PLC injuries are associated with concomitant cruciate ligament tears, as well as meniscal tears and injuries to the medial ligamentous structures.
- In studies to evaluate the outcomes of nonsurgical management with early mobilization in patients who sustained PLC injuries, good results were reported for those patients with grade I and grade II LCL injuries.
- The ramifications of undiagnosed grade III PLC injury include not only recurrent instability and accelerated osteoarthritis but also failed anterior cruciate ligament reconstruction due to increased graft forces caused by loading.
- Certain osseous injuries provide diagnostic clues to an underlying PLC injury that alert the radiologist to closely inspect this region. Avulsion fractures of the fibular head, often referred to as *arcuate fractures* or the *arcuate sign*, occur at the various insertion sites of the PLC components.

Biomechanics, Anatomy, and Injuries of the PLC

The structures of the PLC are primarily responsible for resisting varus angulation—sometimes referred to as *varus rotation*—and external tibial rotation. They act as secondary stabilizers, in conjunction with the cruciate ligaments, to prevent anterior and posterior translation during the early phase of flexion (0°–30°) (1,2).

Initially, the lateral supporting structures of the PLC were divided into three layers (3): The superficial layer was described as consisting of the iliotibial band, its anterior expansion, and the biceps femoris. The middle layer was described as comprising the lateral patellar retinaculum, the two patellofemoral ligaments, and the patellomeniscal ligament. Finally, the deep layer was described as being composed of the lateral capsule, lateral collateral ligament (LCL), coronary ligament (ie, lateral meniscotibial ligament), arcuate ligament, popliteus muscle-tendon unit, popliteofibular ligament (PFL), and fabellofibular ligament.

Our understanding of the PLC has since evolved such that the focus is now on individual structures that work both in isolation and in concert to provide static and dynamic stability to the joint, rather than on structures that are grouped into anatomic compartments. Therefore, to simplify this complex anatomy, we herein describe the most critical structures of the PLC, with an emphasis on the three main stabilizers: the LCL, popliteus tendon, and PFL (Fig 1) (4,5). The interplay and complementary roles of the tendons and ligaments of the PLC are largely due to their anatomic relationships and the close proximity of their insertions onto the fibular head (6); this anatomy is best illustrated in Figure 2. An injury to any one structure alters the synergistic interactions of

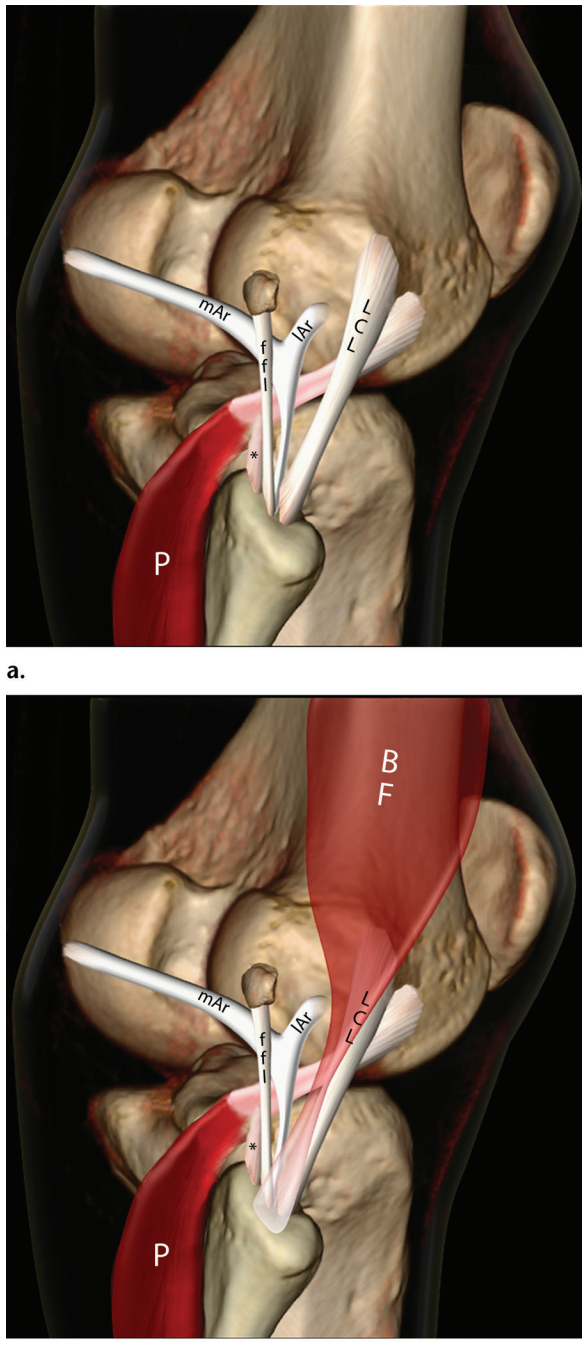

Figure 1. Computer-generated illustrations show the components of the PLC with the biceps femoris *(BF)* removed **(a)** and retained **(b)**. The popliteus muscle *(P)* is the deepest structure, with its tendon coursing under the medial *(mAr)* and lateral *(lAr)* limbs of the arcuate ligament, the fabellofibular ligament *(ffl),* and the LCL to insert onto the femur. The PFL (*) originates from the myotendinous junction of the popliteus tendon and inserts onto the medial aspect of the fibular styloid process.

the components of the PLC and diminishes the ability of the knee to resist varus and external rotational forces.

Lateral Collateral Ligament

The LCL, or fibular collateral ligament, is the primary static restraint to varus stress on the knee and has a secondary role of limiting external rotation, particularly during the early phase of flexion, which peaks at 30° (7). LaPrade and Terry (8) reported injuries of the LCL in 23% of patients who had posterolateral rotational instability at the time of surgery. The LCL, an extracapsular structure, originates from a small osseous depression that is located, on average, 1.4 mm proximal and 3.1 mm posterior to the lateral femoral epicondyle and immediately anterior to the femoral attachment of the lateral head of the gastrocnemius tendon (5). It extends distally in a posteriorly directed fashion to insert onto the lateral aspect of the fibular head, anterior and distal to the fibular styloid process, and it may merge with the distal biceps femoris tendon to form a conjoined structure.

At magnetic resonance (MR) imaging, the LCL is consistently seen as a low-signal-intensity band coursing from the lateral aspect of the distal femur to the lateral aspect of the proximal fibula (Figs 3, 4). Although the J-shaped bursa interposed between the LCL and distal biceps femoris tendon is described in cadaveric studies, it is not readily visualized with imaging (9). Injuries, however, are well depicted with MR imaging (Fig 5). They are typically best characterized in the axial and coronal planes and include soft-tissue avulsions from the femoral and fibular attachment sites; complete or partial intrasubstance tears; periligamentous edema resulting from a sprain; osseous avulsion from the fibular head; and, in the setting of a chronic injury, thickening of the ligament.

Popliteus Musculotendinous Complex

The popliteus musculotendinous complex—consisting of the popliteus tendon, popliteus muscle, and PFL—provides dynamic and static resistance to external rotation, assuming a major role with higher degrees of knee flexion, and acts as a secondary restraint to posterior translation in support of the more dominant posterior cruciate ligament (10,11).

The popliteus muscle arises from the posteromedial aspect of the proximal tibia, above the soleal line, forming a tendon as it ascends laterally. The popliteus tendon runs deep to the arcuate and fabellofibular ligaments, enters the joint through the popliteal hiatus, and courses under and anterior to the LCL to insert onto the anterior fifth portion of the popliteus sulcus of the lateral femoral condyle (5,12,13). This tendon often consists of two bundles: a posterior bundle, which is taut in extension, and an anterior bundle, which is taut in flexion (14). The tendinous portion, which is typically readily identified on MR images, is hypointense, and the muscular component is intermediate in signal intensity (Figs 3, 4). Injuries may occur along any portion of the popliteus musculotendinous complex (Fig 6) but most

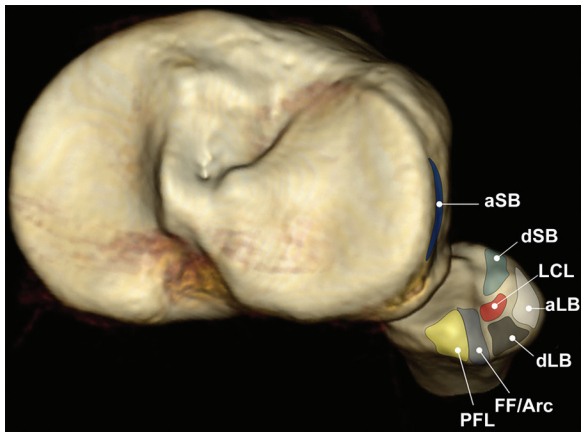

Figure 2. Computer-generated illustration of the proximal tibia and fibula, with the femur removed, demonstrates the insertions of the ligaments and tendons of the PLC. The short head of the biceps femoris tendon divides into an anterior arm *(aSB),* which attaches to the lateral tibial condyle, and a direct arm *(dSB),* which inserts onto the fibula. The LCL is centrally located, with the anterior *(aLB)* and direct *(dLB)* arms of the long head of the biceps femoris tendon attaching onto the lateral aspect of the fibular head. The PFL, arcuate ligament *(Arc),* and fabellofibular ligament *(FF)* attach to the fibular styloid process.

Figure 3. Normal LCL in a 24-year-old man. Coronal proton-density–weighted MR image shows the LCL (arrow) extending from just posterior to the femoral epicondyle to the lateral aspect of the fibular head, where it merges with the biceps femoris tendon. The popliteus tendon (arrowhead) underlies the LCL at the level of the popliteus sulcus.

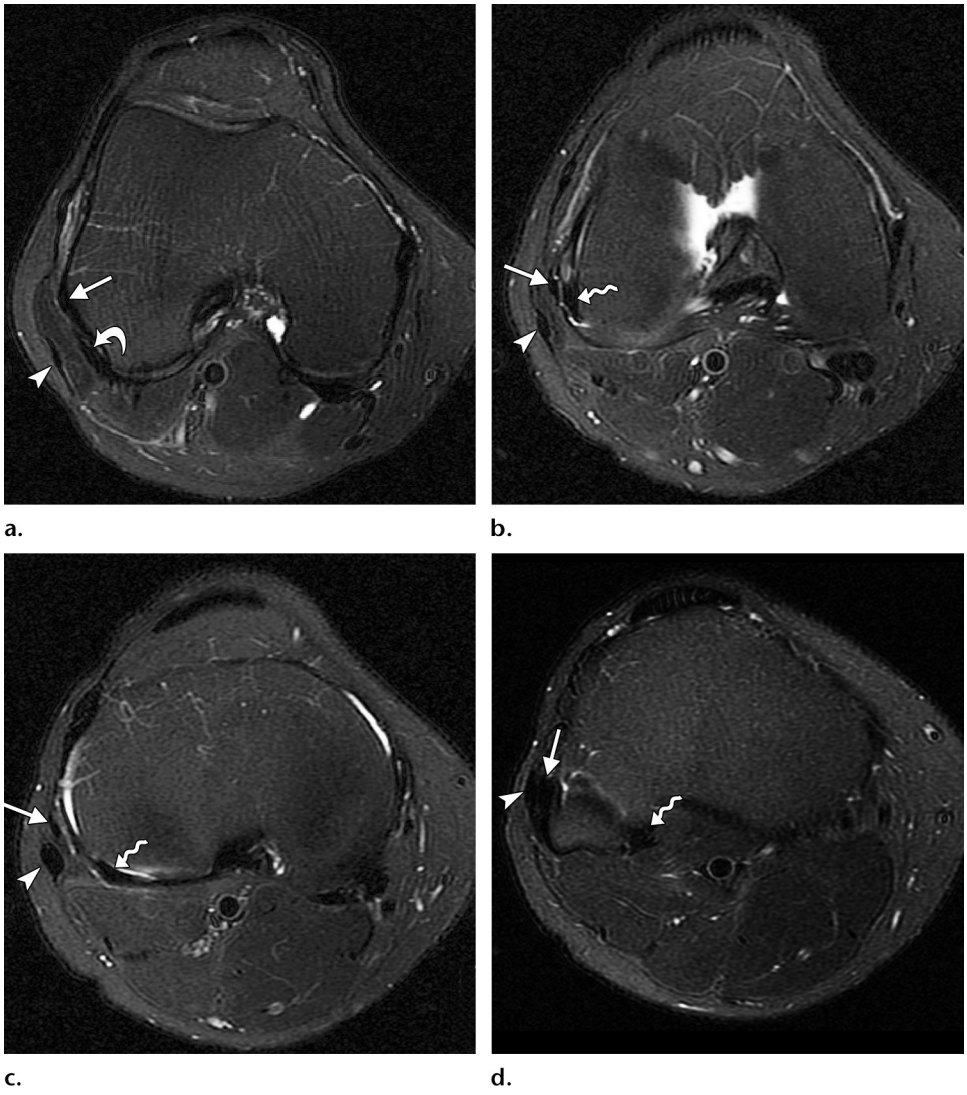

Figure 4. Normal LCL in a 21-year-old man. Consecutive axial T2-weighted fat-suppressed MR images show the normal course and MR imaging appearance of the LCL (straight arrow), biceps femoris tendon (arrowhead), and popliteus tendon (wavy arrow in **b–d**). The origin of the LCL is immediately anterior to the femoral attachment of the lateral head of the gastrocnemius tendon (curved arrow in **a**).

commonly involve the myotendinous junction and are classified as strains, partial tears, or complete tears (15). Imaging has a vital role in the diagnosis and treatment management of high-grade myotendinous injuries of the popliteus musculotendinous complex owing to inherent difficulties in visualizing this region with arthroscopy and the challenge in detecting these injuries clinically, since they are commonly associated with a complex PLC injury that often "clouds" the clinical picture. Avulsion of the tendon at the femoral attachment can occur, and the presence or absence of an attached osseous fragment should be reported, as this may alter the surgical technique used. A cyamella, a rare sesamoid bone found in the popliteus tendon, should not be mistaken for an avulsion fracture or fabella (16).

Ligamentous fascicles (ie, popliteomeniscal fascicles) connect the popliteus tendon to the posterior horn of the lateral meniscus, forming portions of the popliteal hiatus and limiting excessive motion of the lateral meniscus during knee extension (17,18). Although debate regarding the exact number of popliteomeniscal fascicles continues, the posterosuperior and anteroinferior fascicles are routinely identified on sagittal MR images (Fig 7), forming the roof and floor of the popliteal hiatus, respectively (19). Disruption of the posterosuperior popliteomeniscal fascicle (Fig 7b) has a reported positive predictive value of 79%–100% in the diagnosis of arthroscopically confirmed tears of the posterior horn of the lateral meniscus (20).

Originating from the popliteus tendon just proximal to the myotendinous junction and inserting onto the anterior downslope of the medial aspect of the fibular styloid process, the PFL is a stout tendinous band that has recently garnered increased attention because of its role as a major stabilizer of the PLC (21–23). Despite being identified in 93%–100% of cadaveric specimens and having a cross-sectional area similar to that of the popliteus tendon, the PFL remains deceptively difficult to visualize

a.

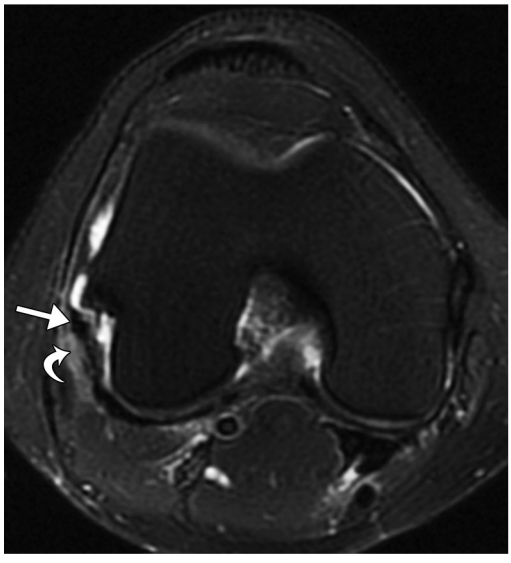

b.

c.

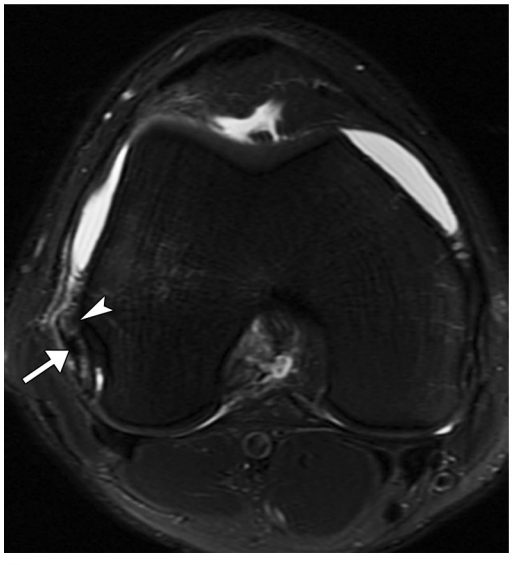

d.

e.

Figure 5. Injuries of the LCL. **(a, b)** Coronal proton-density–weighted **(a)** and axial T2-weighted **(b)** fat-suppressed MR images in a 19-year-old female soccer player show an intact LCL (straight arrow) with periligamentous edema (curved arrow in **b**), which is consistent with a strain (ie, grade I injury). **(c, d)** Coronal proton-density–weighted **(c)** and axial T2-weighted **(d)** fat-suppressed MR images in a 28-year-old man show a partial tear (ie, grade II injury) of the LCL (arrow), as evidenced by the increased intrasubstance signal intensity and indistinctness of the anterior fibers of the proximal portion of the ligament (arrowhead in **d**). **(e)** Coronal proton-density–weighted fat-suppressed MR image in a 25-year-old man shows complete tears (grade III injuries) of both the LCL (arrow) and the biceps femoris tendon (arrowhead), which are avulsed from the fibula.

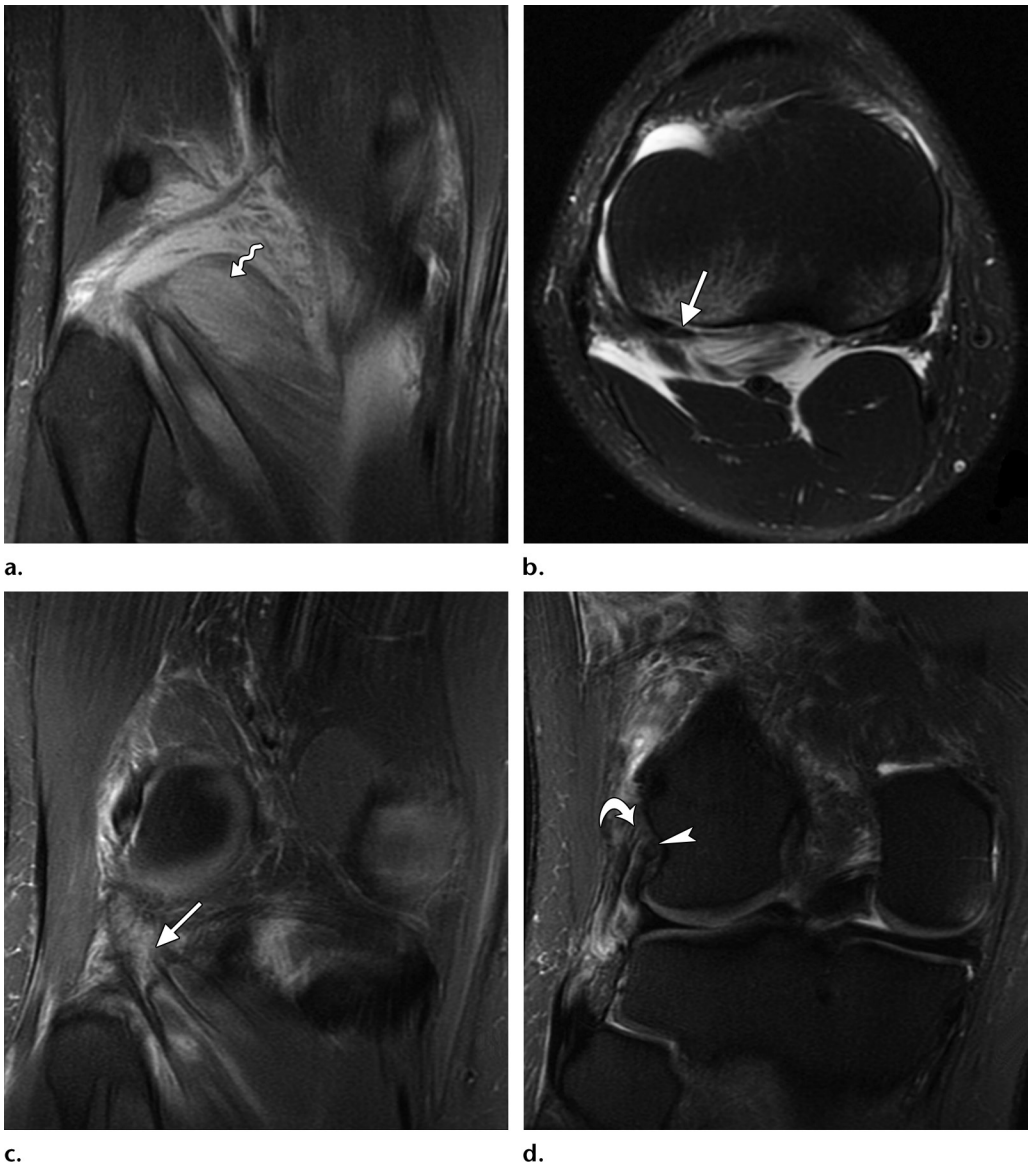

Figure 6. Popliteus injuries. **(a, b)** Coronal proton-density–weighted **(a)** and axial T2-weighted **(b)** fat-suppressed MR images in a 17-year-old boy show a popliteus muscle strain, with intramuscular edema (arrow in **a**) extending to the myotendinous junction (arrow in **b**). **(c, d)** Coronal proton-density–weighted fat-suppressed MR images in a 31-year-old man show a more severe injury involving the myotendinous junction of the popliteus (arrow in **c**), in addition to a partial tear at the insertion of the popliteus tendon (arrowhead in **d**). The patient also sustained a partial tear at the origin of the LCL (curved arrow in **d**).

with conventional knee MR imaging sequences (4,23). Yu et al (24) reported increased visualization of the PFL, from 8% to 53% of cases, with use of a coronal oblique plane oriented perpendicular to the popliteus tendon, compared with visualization of this ligament with use of standard coronal MR imaging sequences. In a more recent study, the use of an isotropic three-dimensional water excitation double-echo steady-state MR imaging sequence, as compared with a coronal oblique T2-weighted fat-saturated MR imaging sequence, improved visualization of the PFL from 71% to 91% of cases (25). However, these MR imaging sequences are not routinely used in practice. In our experience, this ligament is best assessed in the coronal (Fig 8) and sagittal planes, deep to the inferior lateral genicular vessels.

Injuries to the PFL seen on MR images include avulsions from the fibular styloid process; partial tears, which typically appear as increased intrasubstance or peritendinous signal intensity (Figs 8, 9); and ligament disruption. Results during biomechanical testing demonstrated a predictable pattern of sequential failure of the three major stabilizers of the PLC, with compromise of the LCL, followed by the PFL, and finally the popliteus tendon. In the setting of a

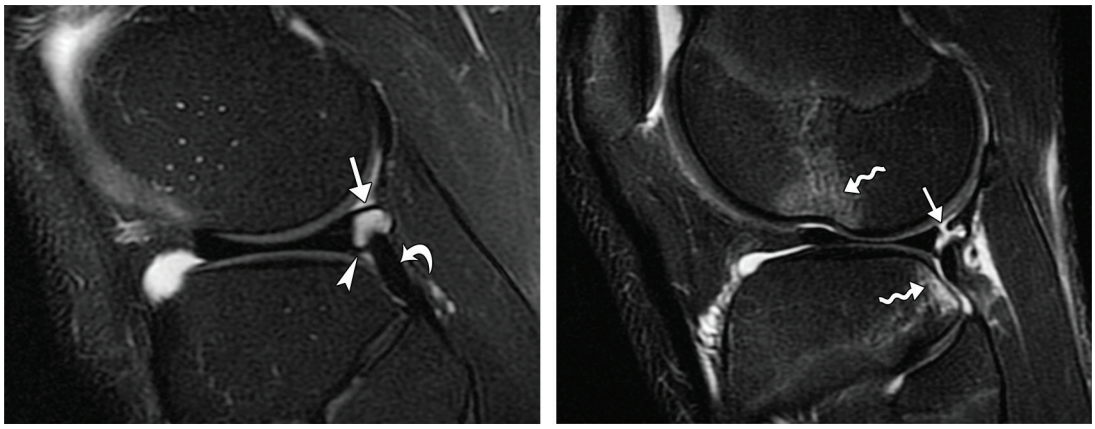

a. b.

Figure 7. Popliteomeniscal fascicles. **(a)** Sagittal T2-weighted fat-suppressed MR image in a 25-year-old man shows the normal posterosuperior (straight arrow) and anteroinferior (arrowhead) popliteomeniscal fascicles forming the roof and floor of the popliteus hiatus, respectively. The popliteus tendon (curved arrow) is seen as it begins its course into the hiatus. **(b)** Sagittal T2-weighted fat-suppressed MR image in a 33-year-old man shows a torn posterosuperior popliteomeniscal fascicle (straight arrow). This injury has a high association with tears involving the posterior horn of the lateral meniscus. The patient also suffered an anterior cruciate ligament injury (not shown), with associated "kissing" contusions (wavy arrows) involving the lateral femoral condyle and posterior aspect of the lateral tibial plateau.

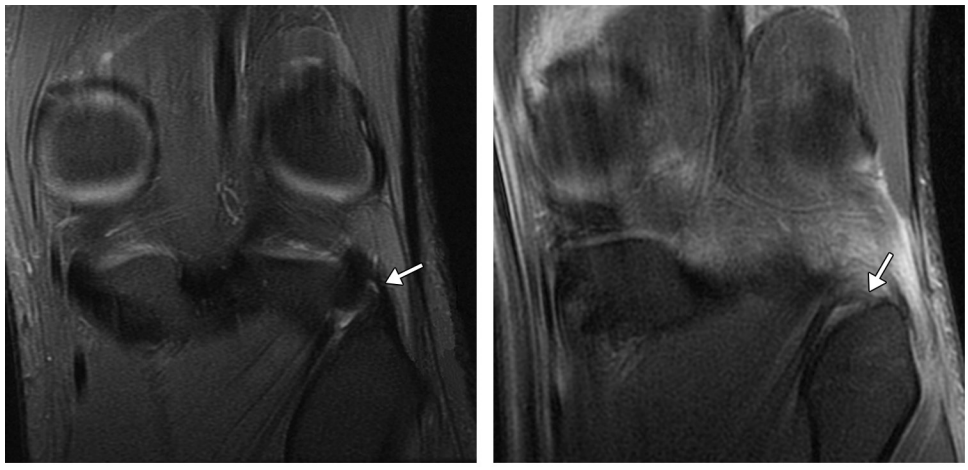

a. b.

Figure 8. Normal PFL and PFL tear. **(a)** Coronal proton-density–weighted fat-suppressed MR image in a 27-year-old woman shows an intact PFL (arrow) extending from the myotendinous junction of the popliteus to the medial aspect of the fibular styloid process. **(b)** Coronal proton-density–weighted fat-suppressed MR image in a 20-year-old man shows, in contrast, increased intrasubstance signal intensity within the PFL (arrow) and surrounding soft-tissue edema, which are consistent with a partial tear.

ruptured PFL, surgical reconstruction is currently advocated to restore normal tibiofemoral stability and kinematics.

Arcuate and Fabellofibular Ligaments

The presence, size, and contributions of the arcuate and fabellofibular ligaments are inversely related. Their detection at cadaveric dissection and MR imaging is quite variable, making recognition of injuries a diagnostic challenge. Arcuate and fabellofibular ligaments appear as thin hypointense bands on MR images (Fig 10), and the use of a coronal oblique plane can substantially improve visualization. Increases in the visualization of these ligaments to nearly 50% of cases have been reported (24).

The arcuate ligament can be viewed as a thickening or reinforcement of the posterolateral capsule (26,27). It has an inverted *Y* configuration, with the medial and lateral limbs attaching to the apex of the fibular styloid process, just lateral to the PFL. The lateral (upright) limb runs superiorly along the joint capsule on its way to the lateral femoral condyle. The medial, or arcuate, limb courses in a superomedial direction, crossing over the popliteus tendon to merge with the posterior capsule and oblique popliteal ligament. The identification of at least one limb in 48%–71% of

Figure 9. Avulsed PFL in a 19-year-old man. **(a, b)** Sagittal T2-weighted **(a)** and coronal proton-density–weighted **(b)** fat-suppressed MR images show avulsion of the PFL (arrow), with associated underlying bone marrow edema (arrowhead) along the medial aspect of the fibular styloid process. **(c)** Sagittal T2-weighted fat-suppressed MR image demonstrates a concomitant injury to the posterior cruciate ligament (arrow) with a large attached avulsed fracture fragment (arrowhead.) PLC injuries are commonly associated with injuries to other stabilizing structures, particularly the cruciate ligaments. **(d)** Lateral radiograph better depicts both the small avulsion fracture off the fibular styloid process (ie, arcuate fracture) (arrow) at the insertion site of the PFL and the tibial avulsion fracture (arrowhead) at the insertion site of the posterior cruciate ligament.

specimens has been reported in cadaveric studies (4,13,28). Interestingly, the lateral limb is more commonly seen in the absence of the fabella; the converse is true for the medial limb.

The fabellofibular ligament appears as a focal thickening of the distal edge of the capsular arm of the short head of the biceps femoris muscle. It originates from the lateral margin of the fabella (Fig 11) or in the absence of a fabella, from the posterior aspect of the supracondylar process of the femur (28). Regardless of its origin, it runs vertically, parallel to the LCL, to insert onto the tip of the fibular styloid process, lateral to the attachment of the PFL and posterior to the attachment of the biceps femoris tendon.

Even when they are present, the arcuate and fabellofibular ligaments are difficult to visualize on MR images (13). On axial and sagittal MR images, the arcuate ligament may appear as a thin low-signal-intensity structure coalescing with the posterolateral capsule and located deep to the inferior lateral genicular artery, overlying the popliteus tendon (Fig 10). The ligament is typically more conspicuous on non–fat-saturated MR images, as it is surrounded by adipose tissue. Injury can be inferred if one identifies an area of increased pericapsular signal intensity surrounding the posterolateral capsule on fat-suppressed fluid-sensitive MR images. With more severe injuries, disruption of the posterolateral capsule may be identified (Fig 12).

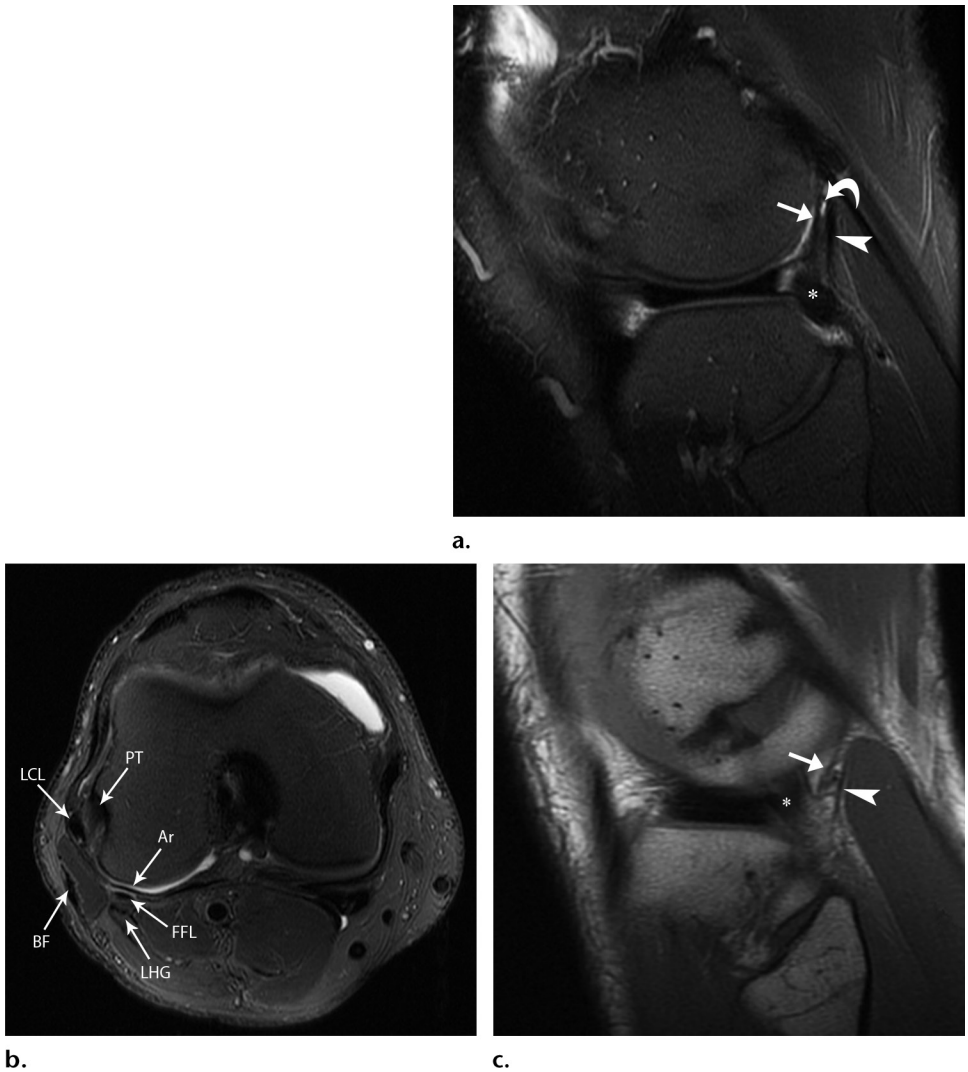

Figure 10. Arcuate and fabellofibular ligaments in a 22-year-old man. **(a)** Sagittal T2-weighted fat-suppressed MR image shows the lateral inferior genicular vessels (curved arrow) coursing between the arcuate (straight arrow) and fabellofibular (arrowhead) ligaments. These vessels serve as an important landmark for localizing these ligaments. The popliteus tendon (*) also can be seen. **(b)** Axial T2-weighted fat-suppressed MR image obtained just above the joint line demonstrates the normal cross-sectional anatomy of the PLC of the knee. *Ar* = arcuate ligament, *BF* = biceps femoris tendon, *FFL* = fabellofibular ligament, *LHG* = lateral head of the gastrocnemius muscle, *PT* = popliteus tendon. **(c)** Sagittal proton-density–weighted non–fat-suppressed MR image lateral to the image in **a** shows the arcuate (arrow) and fabellofibular (arrowhead) ligaments coursing posterior to the popliteus tendon (*). These ligaments are often more conspicuous on non–fat-suppressed MR images, as they are surrounded by adipose tissue.

Assessing the integrity of the fabellofibular ligament is quite challenging and at times not possible. At MR imaging, the ligament is best seen in the coronal or sagittal plane posterior to the arcuate ligament and inferior lateral genicular vessels (Figs 10, 11). On axial MR images, the ligament is seen immediately anterior to the lateral head of the gastrocnemius tendon. The injury patterns seen on MR images (Figs 12, 13) include those of avulsion from the fibular styloid process, partial- and complete-thickness tears, and strains. These injuries often occur in conjunction with an avulsion injury of the direct arm of the short head of the biceps femoris tendon (29).

Biceps Femoris Tendon

Although the biceps femoris tendon is not always included in discussions of the PLC, it deserves mention because it is commonly involved in PLC injuries. The biceps femoris tendon consists of two heads: the long head, which arises from the ischial tuberosity, and the short head, which originates off the lateral prolongation of the linea aspera of the femur. Distally, both heads are composed of at least two tendinous components, a direct arm and an anterior arm, which can be distinguished on MR images in up to 71% of cases (13). The arms of the long head insert onto the anterior and posterolateral

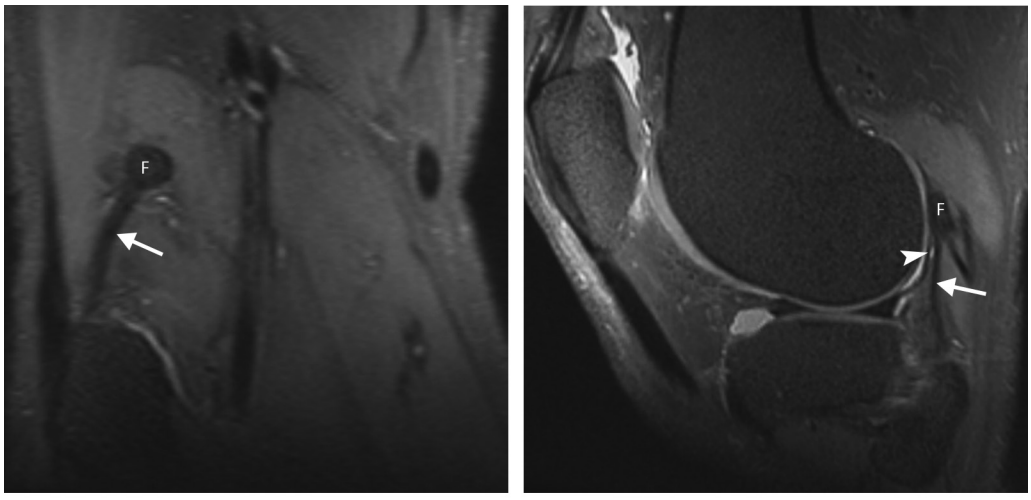

a. b.

Figure 11. Fabellofibular ligament in a 32-year-old man. Reconstructed coronal **(a)** and sagittal **(b)** proton-density–weighted MR images show the fabellofibular ligament (arrow) extending from the fabella *(F)* to the fibular styloid process. The lateral inferior genicular artery (arrowhead in **b**) is seen just deep to the ligament.

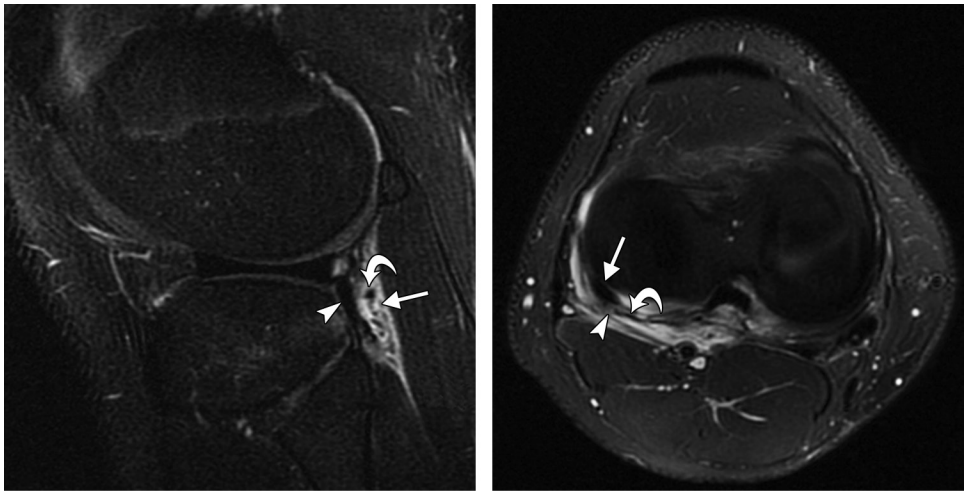

a. b.

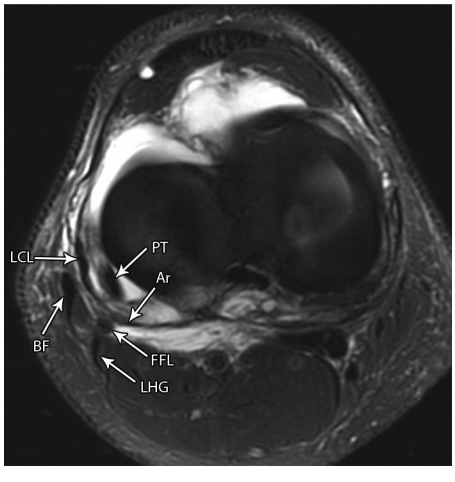

c.

Figure 12. Arcuate ligament injuries. **(a)** Sagittal T2-weighted fat-suppressed MR image in a 28-year-old man shows soft-tissue edema (straight arrow) along the PLC, behind the popliteus tendon (arrowhead) surrounding the lateral inferior genicular artery (curved arrow) in the anatomic location of the arcuate and fabellofibular ligaments. **(b)** Axial T2-weighted fat-suppressed MR image in the same patient shows the arcuate ligament (curved arrow), which is discontinuous (arrowhead) just posterior to the popliteus tendon (straight arrow). **(c)** Axial T2-weighted fat-saturated MR image in a 23-year-old man who has partial tearing of the arcuate *(Ar)* and fabellofibular *(FFL)* ligaments. In this case, the ligaments are intact, with increased intrasubstance signal intensity and periligamentous edema. *BF* = biceps femoris tendon, *LHG* = lateral head of the gastrocnemius muscle, *PT* = popliteus tendon.

aspects of the fibular head, with the anterior arm sending fibers that continue distally as the anterior aponeurosis. The direct arm of the short head inserts onto the anteromedial aspect of the fibular head, while the anterior arm passes medially to the LCL to attach to the superolateral edge of the lateral tibial condyle.

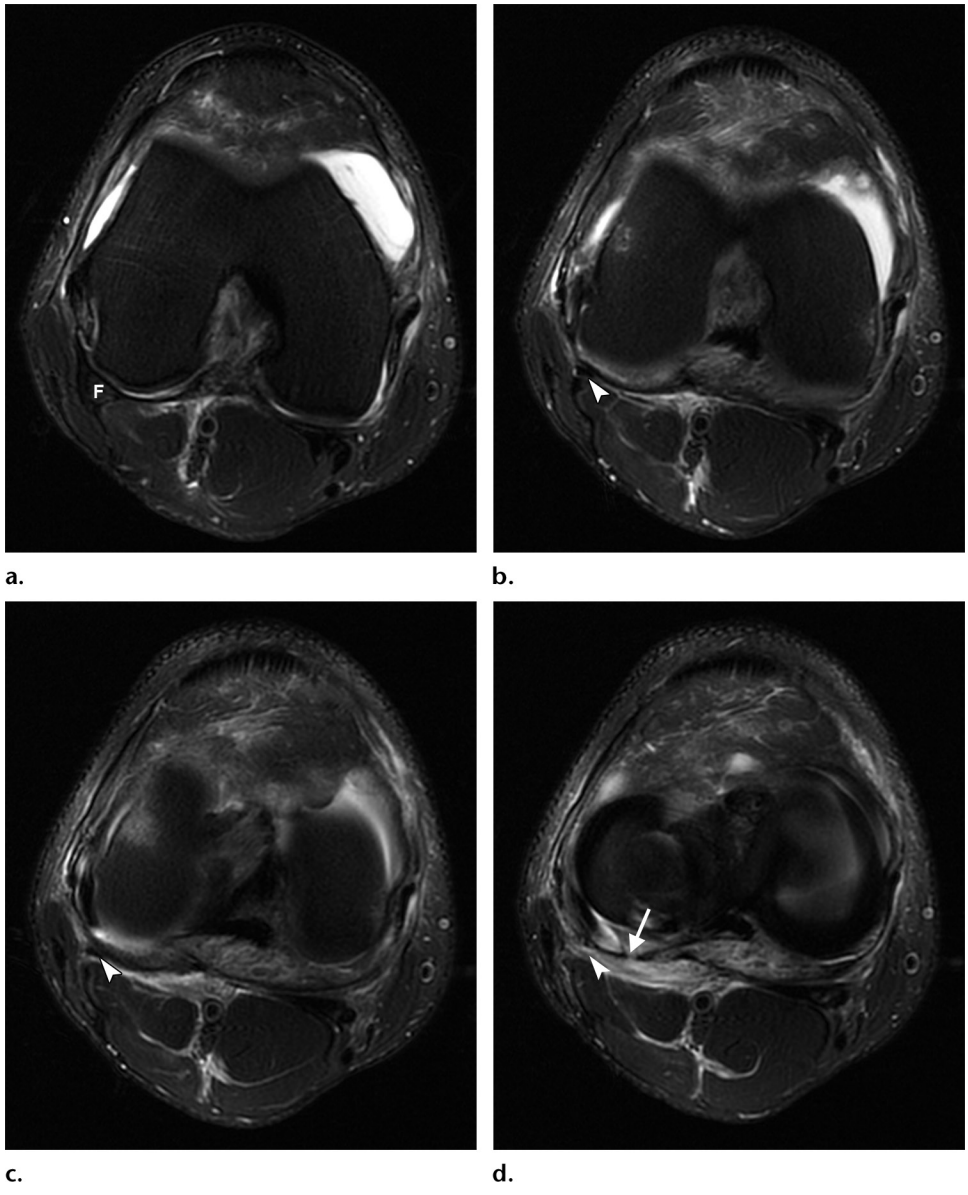

Figure 13. Ruptured fabellofibular ligament in a 31-year-old woman. Serial axial T2-weighted fat-suppressed MR images show the proximal fabellofibular ligament (arrowhead in **b** and **c**) originating from the fabella *(F)*. At the level of the joint line, the fabellofibular ligament is no longer visualized (arrowhead in **d**) where there is soft-tissue edema along the PLC of the knee and focal disruption of the arcuate ligament (arrow in **d**).

At MR imaging, several tendon slips of the biceps femoris tendon can appear to represent a single unit and potentially merge with the distal LCL to form a conjoined structure. Coronal and axial MR images best depict injuries to the biceps femoris tendon, which include tendinous and osseous avulsion from the fibular head; tears of the myotendinous junction; and more subtle partial tears, which have intrasubstance or peritendinous high signal intensity on fluid-sensitive MR images (Figs 5, 14).

Mechanisms of Injury, Clinical Features, and Management of PLC Injuries

Injuries of the PLC are relatively uncommon, occurring in approximately 16% of all knee injuries (30). They are most commonly the result of a posterolaterally directed blow to the anteromedial aspect of the proximal tibia with the knee in full extension (31). Other less common mechanisms include posterior rotatory dislocation (dashboard injury), anterior rotatory dislocation, and hyperextension injury with external rotation (32).

Rarely seen in isolation, the majority of high-grade PLC injuries are associated with concomitant cruciate ligament tears, as well as meniscal tears and injuries to the medial ligamentous structures. Fanelli and Larson (33) reported coexisting PLC injuries in 62% of patients with acute posterior cruciate ligament tears; one should be cognizant of this relationship when interpreting MR imaging findings. Current treatment algorithms are largely based on injury grade, chronicity, and concurrent injuries.

The most common PLC injury classification system, originally proposed by Hughston et al (34), is based on the degree of varus instability at clinical

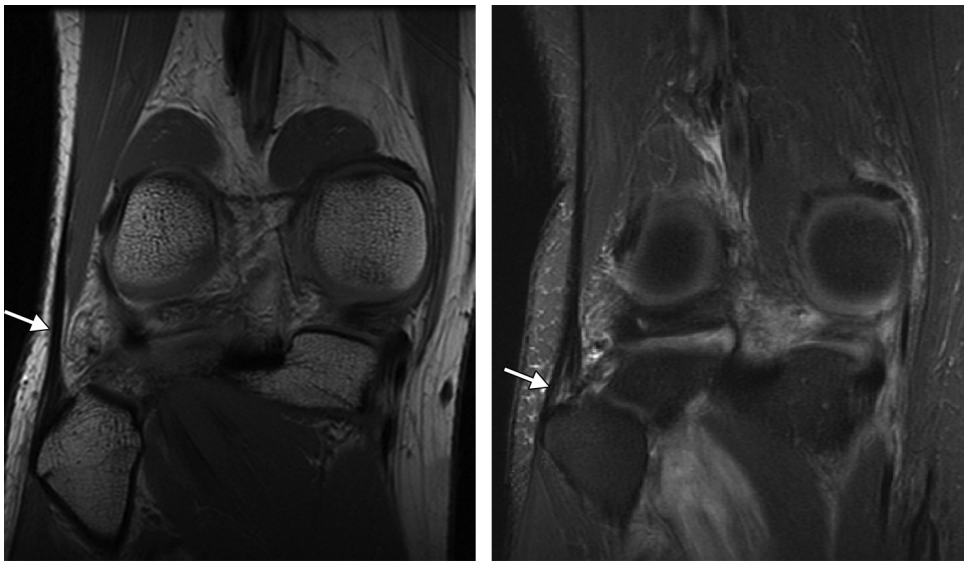

a. b.

Figure 14. Biceps femoris tendon. **(a)** Coronal proton-density–weighted MR image in a 17-year-old girl shows the normal imaging appearance of the distal biceps femoris tendon (arrow). **(b)** Coronal proton-density–weighted fat-suppressed fluid-sensitive MR image in a 22-year-old man shows increased intrasubstance signal intensity and disruption (arrow) of a portion of the fibers of the distal biceps femoris tendon, which are consistent with a partial-thickness tear. Figure 5e shows an avulsed distal biceps femoris tendon.

examination. Grade I injuries are mild sprains that manifest with focal pain along the posterolateral joint line and no clinical findings of laxity (0–5 mm of motion with a definite end point). In comparison, grade II injuries are the result of partial tears and involve mild laxity, which is typically characterized as 6–10 mm of motion and a defined end point. Grade III injuries occur with complete rupture of the capsule-ligamentous structures and involve marked joint laxity (>10 mm of motion), with no appreciable end point detected. The degree of rotational instability is assessed by using the dial test, in which a side-to-side comparison is made to document differences in the thigh-foot angle (10,11). To perform the test, the foot is externally rotated with the knee placed in both 30° and 90° of flexion. At 30° of flexion, increased external rotation of the injured side with an angle difference of 10° or greater compared with the uninjured knee indicates an underlying PLC injury. If the injury is isolated to the PLC, the test will be positive only at 30° of flexion. If, however, increased external rotation persists with the knee positioned at 90° of flexion, then a combined PLC–posterior cruciate ligament injury is present.

In studies to evaluate the outcomes of nonsurgical management with early mobilization in patients who sustained PLC injuries, good results were reported for those patients with grade I and grade II LCL injuries (35,36). Despite having residual laxity, the patients with grade II injuries responded well to conservative management and did not develop radiographic findings of posttraumatic osteoarthritis at a mean follow-up period of 8 years. Conversely, the patients with grade III injuries had poor functional outcomes, persistent instability, and an increased incidence of osteoarthritis in the medial and lateral compartments (35,36).

The ramifications of undiagnosed grade III PLC injury include not only recurrent instability and accelerated osteoarthritis but also failed anterior cruciate ligament reconstruction due to increased graft forces caused by loading (37–40). Therefore, surgical treatment is advocated for patients who have isolated grade III injuries, combined PLC–cruciate ligament injuries, and unsuccessful nonsurgical treatment.

Associated Osseous Injuries

Certain osseous injuries provide diagnostic clues to an underlying PLC injury that alert the radiologist to closely inspect this region. Avulsion fractures of the fibular head, often referred to as *arcuate fractures* or the *arcuate sign*, occur at the various insertion sites of the PLC components (41–43). The most common pattern involves the fibular styloid process, at the attachment of the arcuate complex (ie, popliteofibular, arcuate, and fabellofibular ligaments) (Fig 9). In contrast, fractures resulting from avulsions of the LCL and biceps femoris tendon are larger and involve the lateral margin of the fibular head (Fig 15) (44).

Depending on the size of the avulsed fragment, this type of fracture may be occult on MR

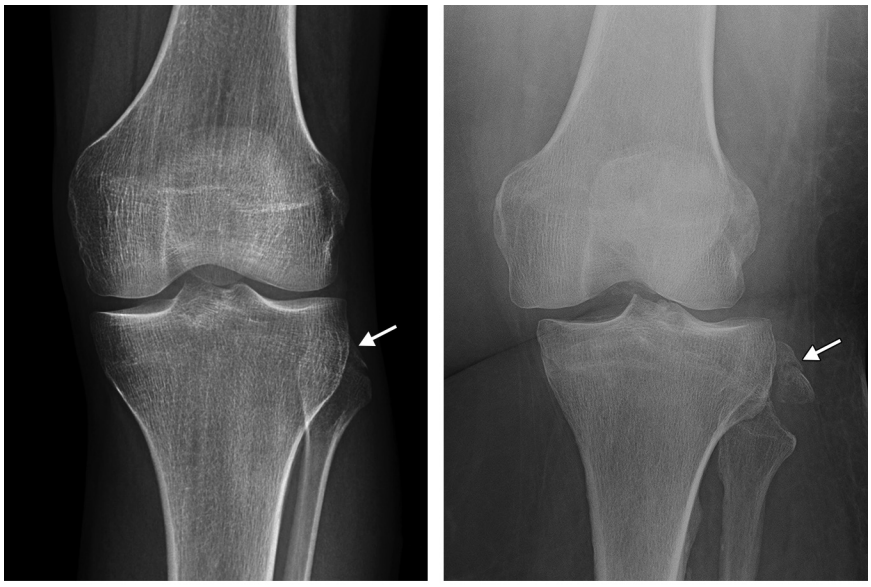

Figure 15. Arcuate fractures. Frontal radiographs of the knee in a 19-year-old man **(a)** and a 37-year-old woman **(b)** show avulsion fractures (arrow) of the fibular head that primarily involve the insertion sites of the LCL and biceps femoris tendon. Lateral translation of the tibia with respect to the femur, which is a secondary sign of instability, is shown in **b**.

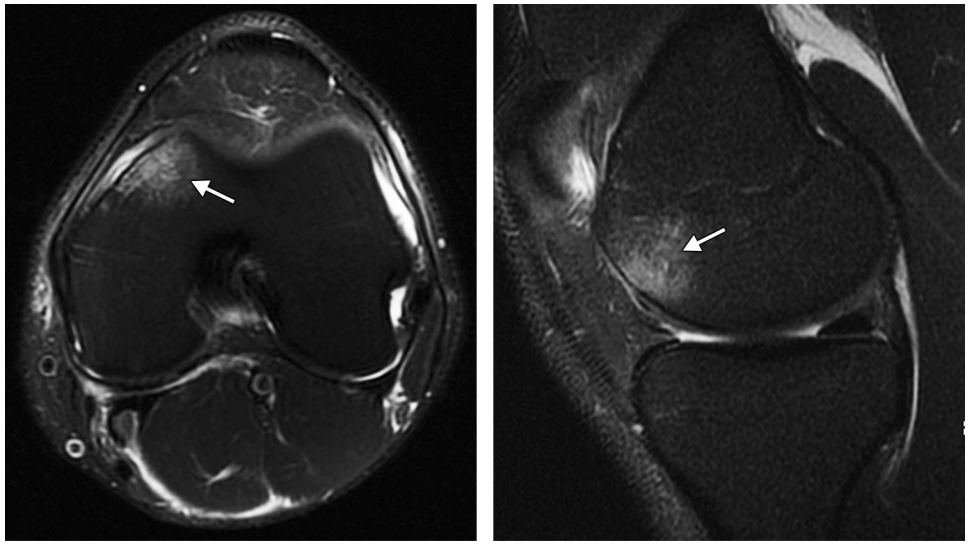

Figure 16. Contusion of the anteromedial femoral condyle in an 18-year-old soccer player who sustained a PLC injury. Axial **(a)** and sagittal **(b)** T2-weighted fat-suppressed MR images show bone marrow edema (arrow) along the anteromedial aspect of the medial femoral condyle. The mechanism of injury was varus force and knee hyperextension.

images, with the only telltale sign being fibular head edema. In this setting, correlation with radiographic findings is essential to identifying small displaced avulsion fractures. In addition to having PLC injuries, patients with arcuate fractures frequently sustain cruciate ligament, medial collateral ligament, and meniscal injuries.

Ross et al (45) reported contusions along the anteromedial femoral condyle (Fig 16) in all patients who had combined grade III PLC injuries and anterior cruciate ligament tears. However, the relatively small sample size of six patients with acute posterolateral knee injuries was a limitation of that study. In one series, a 35% incidence of tibial plateau fractures in patients clinically suspected of having a PLC injury was reported; the majority of these cases involved the anteromedial rim (Fig 17) (46). The suggested mechanism of these uncommon fractures is impaction of the anterior medial femoral condyle into the anteromedial rim of the tibia as a result of varus angulation and posterior translation due to complete disruption of both the PLC and the posterior cruciate ligament.

Finally, Segond fractures (Fig 18) and avulsion of the Gerdy tubercle (Fig 19) also have been associated with PLC injuries (47,48). The Segond fracture is a bone avulsion at the tibial attachment of the mid-third lateral capsular ligament, with

Figure 17. Rim fracture of the anterior medial tibial plateau in a 23-year-old woman who was involved in a motor vehicle collision and presumed dashboard injury and presented with posterolateral rotatory instability. Sagittal computed tomographic (CT) image obtained shortly after the trauma shows a fracture (arrowhead) through the anterior rim of the medial tibial plateau. These rare fractures have a high association with PLC injuries, and owing to the mechanism of injury, they often occur in conjunction with additional osseous injuries. In this case, the patient also sustained a comminuted and depressed fracture involving the posterior aspect of the medial femoral condyle (arrow) owing to direct impact with the anteromedial tibia.

a. **b.**

Figure 18. Segond fracture in a 23-year-old woman following a motor vehicle accident. Frontal radiograph **(a)** and coronal proton-density–weighted fat-suppressed MR image **(b)** show a small displaced fracture fragment (straight arrow) from the lateral proximal tibia at the attachment of the lateral capsular ligament, consistent with a Segond fracture. In addition to a PLC injury (not shown), there are tears of both the anterior cruciate ligament (curved arrow in **b**) and medial collateral ligament (arrowhead in **b**).

potential involvement of the anterior arm of the short head of the biceps femoris tendon. Generally described in association with anterior cruciate ligament injuries, a Segond fracture may also indicate the presence of a concomitant or isolated injury to the PLC. The iliotibial band inserts on the lateral tibia at the Gerdy tubercle, and although rarely injured, both soft-tissue and osseous avulsions have been reported with a complex PLC injury (45).

Role of Imaging and How to Report Findings

Diagnosis of PLC injuries is based on the clinical presentation. In practice, however, the physical examination findings are often dominated by associated injuries, particularly those involving the cruciate ligaments. Imaging, especially MR imaging, has an important role in uncovering unsuspected PLC injuries, as their early detection (ie, <3 weeks before they incite injury) and treatment can result in improved outcomes and potentially obviate additional procedures (21,49).

At MR imaging, injuries can be classified as strains, which primarily involve an intact ligament or tendon with surrounding edema; partial tears, with increased intrasubstance signal intensity and disruption of portions of the muscle, ligament, or tendon; or complete rupture—with these often corresponding to the clinical findings of grade I, II, and III injuries, respectively (Fig 5). Although there are no imaging criteria to distinguish clinically unstable grade III PLC injuries, complete tears of the major stabilizers (ie, popliteus tendon, PFL, and LCL) should be reported as findings suspicious for posterolateral instability, particularly when two or more components are involved or

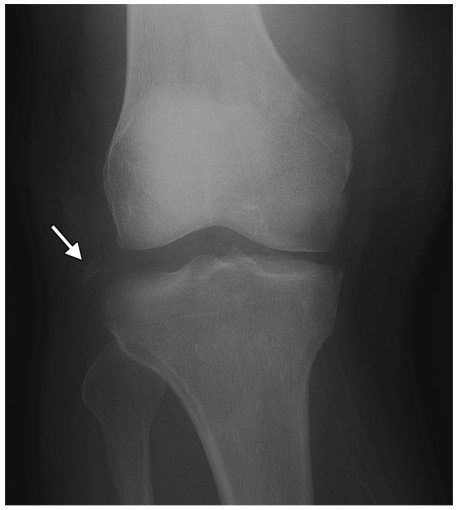

a.

b.

c.

Figure 19. Avulsion fracture of the Gerdy tubercle in a 27-year-old man with a PLC injury. Frontal radiograph **(a)**, coronal multiplanar reconstruction CT image **(b)**, and coronal proton-density–weighted fat-suppressed MR image **(c)** show the avulsion fracture (straight arrow). In **c**, the fragment is seen attached to a retracted and avulsed iliotibial band (arrowhead). The proposed mechanism for this type of injury is pure varus force, which can result in "kissing" contusions (curved arrows) involving the medial femoral condyle and medial tibial plateau, as in this case.

there is a concomitant cruciate ligament injury. In complex knee injuries, these findings may direct the orthopedic surgeon to closely interrogate the PLC complex and, if necessary, perform an examination with use of anesthesia. The statuses of the menisci, cruciate ligaments, medial collateral ligament, hyaline cartilage, and structures of the posteromedial corner of the knee also should be included in the report, as these will affect overall treatment-related decision making. In the setting of a knee dislocation, CT or MR angiography should be performed to assess the popliteal vasculature and nerves.

Conclusion

Although rare, high-grade PLC injuries have devastating consequences—including accelerated osteoarthritis, chronic instability, and failed cruciate ligament reconstruction—if they are not recognized. When interpreting MR imaging findings, a thorough understanding of the normal anatomy, MR imaging appearances, biomechanics, injury patterns, and associated injuries is the foundation for recognizing—and suggesting the diagnosis of—a PLC injury. The role of imaging in early detection of these injuries is particularly important for patients with complex injuries, as the clinical findings can be quite confounding.

References

1. Nielsen S, Rasmussen O, Ovesen J, Andersen K. Rotatory instability of cadaver knees after transection of collateral ligaments and capsule. Arch Orthop Trauma Surg 1984;103(3):165–169.
2. Nielsen S, Ovesen J, Rasmussen O. The posterior cruciate ligament and rotatory knee instability: an experimental study. Arch Orthop Trauma Surg 1985;104(1):53–56.
3. Seebacher JR, Inglis AE, Marshall JL, Warren RF. The structure of the posterolateral aspect of the knee. J Bone Joint Surg Am 1982;64(4):536–541.
4. Watanabe Y, Moriya H, Takahashi K, et al. Functional anatomy of the posterolateral structures of the knee. Arthroscopy 1993;9(1):57–62.
5. LaPrade RF, Ly TV, Wentorf FA, Engebretsen L. The posterolateral attachments of the knee: a qualitative and quantitative morphologic analysis of the fibular collateral ligament, popliteus tendon, popliteofibular ligament, and lateral gastrocnemius tendon. Am J Sports Med 2003;31(6):854–860.
6. Dye SF. An evolutionary perspective of the knee. J Bone Joint Surg Am 1987;69(7):976–983.
7. Sanchez AR 2nd, Sugalski MT, LaPrade RF. Anatomy and biomechanics of the lateral side of the knee. Sports Med Arthrosc Rev 2006;14(1):2–11.

8. LaPrade RF, Terry GC. Injuries to the posterolateral aspect of the knee: association of anatomic injury patterns with clinical instability. Am J Sports Med 1997;25(4):433–438.
9. LaPrade RF, Hamilton CD. The fibular collateral ligament-biceps femoris bursa: an anatomic study. Am J Sports Med 1997;25(4):439–443.
10. Gollehon DL, Torzilli PA, Warren RF. The role of the posterolateral and cruciate ligaments in the stability of the human knee: a biomechanical study. J Bone Joint Surg Am 1987;69(2):233–242.
11. Grood ES, Stowers SF, Noyes FR. Limits of movement in the human knee: effect of sectioning the posterior cruciate ligament and posterolateral structures. J Bone Joint Surg Am 1988;70(1):88–97.
12. De Maeseneer M, Shahabpour M, Vanderdood K, De Ridder F, Van Roy F, Osteaux M. Posterolateral supporting structures of the knee: findings on anatomic dissection, anatomic slices and MR images. Eur Radiol 2001;11(11):2170–2177.
13. Munshi M, Pretterklieber ML, Kwak S, Antonio GE, Trudell DJ, Resnick D. MR imaging, MR arthrography, and specimen correlation of the posterolateral corner of the knee: an anatomic study. AJR Am J Roentgenol 2003;180(4):1095–1101.
14. Perez Carro L, Sumillera Garcia M, Sunye Gracia C. Bifurcate popliteus tendon. Arthroscopy 1999;15(6):638–639.
15. Brown TR, Quinn SF, Wensel JP, Kim JH, Demlow T. Diagnosis of popliteus injuries with MR imaging. Skeletal Radiol 1995;24(7):511–514.
16. Akansel G, Inan N, Sarisoy HT, Anik Y, Akansel S. Popliteus muscle sesamoid bone (cyamella): appearance on radiographs, CT and MRI. Surg Radiol Anat 2006;28(6):642–645.
17. Stäubli HU, Birrer S. The popliteus tendon and its fascicles at the popliteal hiatus: gross anatomy and functional arthroscopic evaluation with and without anterior cruciate ligament deficiency. Arthroscopy 1990;6(3):209–220.
18. Cohn AK, Mains DB. Popliteal hiatus of the lateral meniscus: anatomy and measurement at dissection of 10 specimens. Am J Sports Med 1979;7(4):221–226.
19. Johnson RL, De Smet AA. MR visualization of the popliteomeniscal fascicles. Skeletal Radiol 1999;28(10):561–566.
20. De Smet AA, Asinger DA, Johnson RL. Abnormal superior popliteomeniscal fascicle and posterior pericapsular edema: indirect MR imaging signs of a lateral meniscal tear. AJR Am J Roentgenol 2001;176(1):63–66.
21. Veltri DM, Deng XH, Torzilli PA, Maynard MJ, Warren RF. The role of the popliteofibular ligament in stability of the human knee: a biomechanical study. Am J Sports Med 1996;24(1):19–27.
22. Shahane SA, Ibbotson C, Strachan R, Bickerstaff DR. The popliteofibular ligament: an anatomical study of the posterolateral corner of the knee. J Bone Joint Surg Br 1999;81(4):636–642.
23. Maynard MJ, Deng X, Wickiewicz TL, Warren RF. The popliteofibular ligament: rediscovery of a key element in posterolateral stability. Am J Sports Med 1996;24(3):311–316.
24. Yu JS, Salonen DC, Hodler J, Haghighi P, Trudell D, Resnick D. Posterolateral aspect of the knee: improved MR imaging with a coronal oblique technique. Radiology 1996;198(1):199–204.
25. Rajeswaran G, Lee JC, Healy JC. MRI of the popliteofibular ligament: isotropic 3D WE-DESS versus coronal oblique fat-suppressed T2W MRI. Skeletal Radiol 2007;36(12):1141–1146.
26. Moorman CT 3rd, LaPrade RF. Anatomy and biomechanics of the posterolateral corner of the knee. J Knee Surg 2005;18(2):137–145.
27. Recondo JA, Salvador E, Villanúa JA, Barrera MC, Gervás C, Alústiza JM. Lateral stabilizing structures of the knee: functional anatomy and injuries assessed with MR imaging. RadioGraphics 2000;20(Spec No):S91–S102.
28. Diamantopoulos A, Tokis A, Tzurbakis M, Patsopoulos I, Georgoulis A. The posterolateral corner of the knee: evaluation under microsurgical dissection. Arthroscopy 2005;21(7):826–833.
29. Haims AH, Medvecky MJ, Pavlovich R Jr, Katz LD. MR imaging of the anatomy of and injuries to the lateral and posterolateral aspects of the knee. AJR Am J Roentgenol 2003;180(3):647–653.
30. LaPrade RF, Wentorf FA, Fritts H, Gundry C, Hightower CD. A prospective magnetic resonance imaging study of the incidence of posterolateral and multiple ligament injuries in acute knee injuries presenting with a hemarthrosis. Arthroscopy 2007;23(12):1341–1347.
31. Fornalski S, McGarry MH, Csintalan RP, Fithian DC, Lee TQ. Biomechanical and anatomical assessment after knee hyperextension injury. Am J Sports Med 2008;36(1):80–84.
32. Baker CL Jr, Norwood LA, Hughston JC. Acute posterolateral rotatory instability of the knee. J Bone Joint Surg Am 1983;65(5):614–618.
33. Fanelli GC, Larson RV. Practical management of posterolateral instability of the knee. Arthroscopy 2002;18(2 suppl 1):1–8.
34. Hughston JC, Andrews JR, Cross MJ, Moschi A. Classification of knee ligament instabilities. II. The lateral compartment. J Bone Joint Surg Am 1976;58(2):173–179.
35. Kannus P. Nonoperative treatment of grade II and III sprains of the lateral ligament compartment of the knee. Am J Sports Med 1989;17(1):83–88.
36. Krukhaug Y, Mølster A, Rodt A, Strand T. Lateral ligament injuries of the knee. Knee Surg Sports Traumatol Arthrosc 1998;6(1):21–25.
37. Harner CD, Vogrin TM, Höher J, Ma CB, Woo SL. Biomechanical analysis of a posterior cruciate ligament reconstruction: deficiency of the posterolateral structures as a cause of graft failure. Am J Sports Med 2000;28(1):32–39.
38. O'Brien SJ, Warren RF, Pavlov H, Panariello R, Wickiewicz TL. Reconstruction of the chronically insufficient anterior cruciate ligament with the central third of the patellar ligament. J Bone Joint Surg Am 1991;73(2):278–286.
39. Noyes FR, Barber-Westin SD, Roberts CS. Use of allografts after failed treatment of rupture of the anterior cruciate ligament. J Bone Joint Surg Am 1994;76(7):1019–1031.
40. LaPrade RF, Resig S, Wentorf F, Lewis JL. The effects of grade III posterolateral knee complex injuries on anterior cruciate ligament graft force: a biomechanical analysis. Am J Sports Med 1999;27(4):469–475.
41. Juhng SK, Lee JK, Choi SS, Yoon KH, Roh BS, Won JJ. MR evaluation of the "arcuate" sign of posterolateral knee instability. AJR Am J Roentgenol 2002;178(3):583–588.
42. Shindell R, Walsh WM, Connolly JF. Avulsion fracture of the fibula: the 'arcuate sign' of posterolateral knee instability. Nebr Med J 1984;69(11):369–371.
43. Huang GS, Yu JS, Munshi M, et al. Avulsion fracture of the head of the fibula (the "arcuate" sign): MR imaging findings predictive of injuries to the posterolateral ligaments and posterior cruciate ligament. AJR Am J Roentgenol 2003;180(2):381–387.
44. Lee J, Papakonstantinou O, Brookenthal KR, Trudell D, Resnick DL. Arcuate sign of posterolateral knee injuries: anatomic, radiographic, and MR imaging data related to patterns of injury. Skeletal Radiol 2003;32(11):619–627.
45. Ross G, Chapman AW, Newberg AR, Scheller AD Jr. Magnetic resonance imaging for the evaluation of acute posterolateral complex injuries of the knee. Am J Sports Med 1997;25(4):444–448.
46. Bennett DL, George MJ, El-Khoury GY, Stanley MD, Sundaram M. Anterior rim tibial plateau fractures and posterolateral corner knee injury. Emerg Radiol 2003;10(2):76–83.
47. Dietz GW, Wilcox DM, Montgomery JB. Segond tibial condyle fracture: lateral capsular ligament avulsion. Radiology 1986;159(2):467–469.
48. DeLee JC, Riley MB, Rockwood CA Jr. Acute straight lateral instability of the knee. Am J Sports Med 1983;11(6):404–411.
49. Geeslin AG, LaPrade RF. Outcomes of treatment of acute grade-III isolated and combined posterolateral knee injuries: a prospective case series and surgical technique. J Bone Joint Surg Am 2011;93(18):1672–1683.